Spectrochimica Acta Part B: Atomic Spectroscopy 235 (2026) 107377

Contents lists available at ScienceDirect

Spectrochimica Acta Part B: Atomic Spectroscopy

journal homepage: www.elsevier.com/locate/sab

Overcoming matrix effects on the determination of phosphorus concentration in sewage sludge ash using laser-induced breakdown spectroscopy hand-held instrumentation

Mattia Massa [a,1], Elisa Galli [b,1], Alessandra Zanoletti [a], Annalisa Zacco [a], Silvana De Iuliis [c], Laura Eleonora Depero [a], Vincenzo Palleschi [d], Laura Borgese [a,*], Elza Bontempi [a]

[a] INSTM & Chemistry for Technologies Laboratory, Department of Mechanical and Industrial Engineering, University of Brescia, Via Branze 38, 25123 Brescia, Italy
[b] INSTM and Department of Information Engineering, Chemistry and Sustainable Materials Laboratory, University of Brescia, Via Branze 38, Brescia 25123, Italy
[c] Institute of Condensed Matter Chemistry and Energy Technologies, National Research Council, Milano, Italy
[d] Institute of Chemistry of Organometallic Compounds, National Research Council, Pisa, Italy

ARTICLE INFO

Keywords:
Laser induced breakdown spectroscopy
Phosphorus recycle
Sewage sludge ash
Hand-held LIBS
Deep learning
Convolutional neural networks

ABSTRACT

Sewage sludge ash (SSA), derived from the incineration of wastewater treatment sludge, typically contains phosphorus concentrations ranging from 4 % to 12 % by weight. This significant P content makes SSA a promising secondary resource, particularly for applications such as fertilizer production. In this study, we explore the feasibility of using handheld Laser-Induced Breakdown Spectroscopy (LIBS) for the rapid and direct determination of phosphorus content in SSA samples. The proposed method enables rapid and accurate quantification of phosphorus with minimal sample preparation and demonstrates strong resilience to matrix effects, which often compromise the reliability of conventional LIBS analysis.

The approach is based on a Convolutional Neural Network (CNN), designed to produce a single calibration model capable of addressing the wide variability in phosphorus concentration typically observed in SSA samples. The innovative aspect of this work is the complete separation of the training stage of the CNN, which is done using simple synthetic reference samples, from the validation, which involves actual SSA samples collected from a waste-to-energy power plant, previously characterized using standard laboratory methods. This procedure allows to select, among the many spectral features that can be used for modelling the training set, only the ones that are proven to effectively work for the determination of phosphorous concentration in the SSA samples, which have a much more complex composition with respect to the synthetic training samples.

In addition to presenting this novel methodology, the study also includes a discussion of alternative approaches reported in the literature for matrix-independent quantitative LIBS analysis of phosphorus. This comparative overview highlights the advantages of the proposed method for in-situ analysis of SSA.

1. Introduction

Phosphorus plays a fundamental role in ensuring global food security, as it is a non-substitutable component in fertilizers, and it is widely used in a broad range of industrial and technological sectors. Due to the high risk of supply disruption and its essential function, phosphorus has been officially included by the European Commission in the list of Critical Raw Materials. Sewage sludge ash (SSA), obtained from the thermal treatment of wastewater treatment residuals, has emerged as a promising secondary source of phosphorus. SSA contains phosphorus at concentrations between 4 % and 12 %, comparable to those found in low-grade phosphate rock [1,2]. Standardized methods such as Inductively Coupled Plasma Optical Emission Spectroscopy (ICP-OES) or Mass Spectrometry (ICP-MS) are commonly employed for the determination of P content, especially in the context of waste characterization. ICP based techniques are highly sensitive and capable of detecting a wide range of elements with excellent accuracy. However, they require complete solubilization of the sample or analyte extraction that can be particularly challenging for waste-derived materials, whose heterogeneous and complex composition may lead to incomplete dissolution of

* Corresponding author.
E-mail address: laura.borgese@unibs.it (L. Borgese).
[1] These authors contributed equally.

https://doi.org/10.1016/j.sab.2025.107377
Received 28 August 2025; Received in revised form 24 October 2025; Accepted 27 October 2025
Available online 29 October 2025

certain mineral phases. As a result, this can compromise the accuracy and representativeness of the analytical results. The recovery of phosphorus from SSA requires a clear understanding of its total content and chemical speciation, since P in these matrices is often found in mineral forms (e.g., calcium phosphates or whitlockite-like structures), some of which are poorly soluble and resistant to classical extraction methods [3]. In many cases, achieving acceptable recovery yields requires the use of strong acids under extremely low pH conditions, along with large volumes of hazardous reagents, raising concerns about safety, cost, environmental sustainability, and waste generation [4]. In this regard, the direct analysis of phosphorus in ash becomes a strategically sustainable alternative. This can allow for rapid, accurate, and non-destructive quantification of phosphorus, eliminating the need for sample digestion. It not only simplifies the analytical workflow but also aligns with the principles of green chemistry by reducing the use of aggressive chemicals and minimizing laboratory waste, according to a brief quantitative sustainability assessment using the AGREE metric (default weighting over the 12 Green Analytical Chemistry principles) [5].

Laser-Induced Breakdown Spectroscopy (LIBS) and X-Ray Fluorescence (XRF) are two widely used techniques for direct elemental analysis of solid samples with minimal or no sample preparation, each offering distinct advantages depending on the application context. XRF uses an X-ray beam to excite the atoms in the sample, which then emit secondary (fluorescent) X-rays that are specific to each element. This method is fully non-destructive and extremely reliable for quantifying medium and heavy elements (e.g., Cu, Zn, Pb) with high precision and reproducibility. However, its sensitivity to light elements such as phosphorus is limited under ambient conditions due to the strong absorption of low-energy X-rays in air and matrix effects [6]. LIBS operates by focusing a high-energy laser pulse onto the sample surface, creating a micro plasma that emits light characteristic of the elements present. One of LIBS' main advantages is its ability to perform in situ, making it highly suitable for process monitoring and field applications. Its micro-destructive nature, although negligible for most practical purposes, also distinguishes it from completely non-invasive techniques [7]. One of the most significant advancements in LIBS technology has been the introduction of handheld instruments [8], which have narrowed the gap for in-situ usability compared to other powerful analytical techniques, such as X-Ray Fluorescence XRF.

With respect to XRF, LIBS enables the detection of both light and heavy elements, including phosphorus, with greater flexibility in handling irregular or inhomogeneous samples. Nevertheless, LIBS suffers from matrix-dependent signal variations and generally requires advanced calibration models (e.g., multivariate regression or machine learning) and matrix-matched standards to achieve quantitative accuracy [9]. These effects stem from changes in the main plasma parameters, such as total ablated mass, electron temperature, and electron number density, which directly influence the LIBS spectral emission. Variations in matrix composition, due to differences in physical and chemical properties between samples, can lead to inconsistencies in these parameters. For instance, surface morphology can affect laser energy absorption and, consequently, the ablated mass, while changes in chemical structure can impact the evolution of plasma thermodynamic parameters.

As a result, traditional LIBS analysis using calibration curves is often complicated by non-linear and sometimes non-monotonic relationships between the emitted signal intensity and analyte concentration. This strong sensitivity to matrix effects is, paradoxically, a consequence of LIBS's broad dynamic range, which allows for the detection of elemental concentrations spanning from a few parts per million to several tens of percent. Consequently, the reference materials used to build conventional calibration curves often differ significantly in matrix composition, introducing additional variability.

One of the main sources of matrix effects in LIBS is the variation in ablated mass caused by physical changes to the sample surface (e.g., reflectivity, hardness) that occur due to changes in elemental concentration. To mitigate this effect, the analyte signal is normalized to the intensity of a spectral line from an internal standard—an added element of known concentration not originally present in the sample. This yields a result proportional to the analyte-to-standard concentration ratio, effectively correcting for variations in ablated mass. This approach does not correct for changes in plasma properties such as electron temperature and number density, unless the internal standard coincidentally has an ionization energy and emission line characteristics (e.g., upper-level energy of the transition) very similar to those of the analyte. A simpler yet effective method for reducing physical matrix effects is normalizing the analyte LIBS signal to the spectral continuum background or to the total integrated intensity of the spectrum, which serve as approximate proxies for the total ablated mass [10].

Focusing on the specific topic of this paper, matrix effects in LIBS analysis of phosphorus-rich samples have been addressed in two studies, each adopting a distinct approach. In 2022, Elsayed et al. [11] proposed the use of a Calibration-Free LIBS (CF-LIBS) approach for determining phosphorus content in phosphogypsum waste. CF-LIBS, initially introduced by Ciucci et al. [12], is a standard-less analytical method that assumes a homogeneous plasma under local thermal equilibrium (LTE) conditions [13]. The method derives plasma parameters (e.g., temperature and electron number density) directly from the LIBS spectrum and uses these to correct for matrix effects, enabling a composition determination that is largely matrix independent [9]. CF-LIBS is particularly suitable for analyzing waste materials with highly variable composition [14]. However, one key limitation is that CF-LIBS requires time-resolved spectrometry, since laser-induced plasmas evolve rapidly and LTE conditions are only satisfied during a narrow temporal window in the plasma's lifetime. Accurate results thus require measurements within this window, that must be short enough to avoid significant variations in plasma conditions. Unfortunately, this requirement is incompatible with the design and operational constraints of handheld LIBS devices, which typically lack time-resolved detection capabilities. Some methods have been proposed to extract time-resolved information from time-integrated LIBS spectra [15,16], but these generally involve more complex and time-consuming procedures (e.g., acquiring spectra at multiple delay times), making CF-LIBS unsuitable for fast, on-site phosphorus analysis using handheld instrumentation.

A second study addressing matrix effects in phosphorus-rich mineral supplements for cattle was conducted by Babos et al. [17]. The phosphorus concentrations ranged from 3 % to 12 %, aligning well with typical SSA values. The authors proposed two strategies, one of which is the Multi-Energy Calibration (MEC) method [18]. In principle, this method requires only one reference sample of known composition and one "blank" (i.e., a sample with zero analyte concentration) to determine phosphorous concentrations in samples with unknown concentrations. The MEC approach involves preparing two mixtures: one composed of 50 % (by weight) of the standard and 50 % of the blank, and the second of 50 % of the standard and 50 % of the sample to be analyzed. Alternative mixing ratios may be used depending on the specific application. The LIBS intensities of two or more phosphorus lines are recorded by analyzing both mixtures under identical experimental conditions. For each line, the signal of the "standard+blank" mixture is plotted on the x-axis (as a function of line energy), and the corresponding signal of the "standard+unknown" mixture is plotted on the y-axis. Assuming a linear relationship between the LIBS signal and analyte concentration, the data points are expected to fall along a straight line with slope S, which can then be used to determine the analyte concentration in the unknown sample.

The MEC procedure is essentially a variation of the traditional single-standard calibration method. Indeed, any calibration approach based on a single reference standard inevitably encounters the same well-known limitations, which have been discussed extensively in literature over the past decades. Furthermore, the method does not account for potential matrix effects since the derivation of Eq. (1) relies on the assumption of

the same proportionality of the LIBS signal on the analyte concentration in both the standard and the unknown sample.

A similar limitation applies to the second method proposed in ref. [17], known as one-point gravimetric standard addition [19]. In this method, two samples are prepared by mixing equal parts by weight (50 %) of the standard with either the blank or the unknown sample. Only one emission line of the analyte is used. Let $I_{(S+B)}$ be the intensity of the emission line measured in the standard+blank mixture, and $I_{(S+Unk)}$ the intensity measured in the standard+unknown mixture. The analyte concentration in the unknown sample is then given by:

$$C_{unk} = C_s \left(\frac{I_{S+Unk}}{I_{S+B}} - 1 \right) \quad (1)$$

As with the MEC method, Eq. (1) assumes linearity of the LIBS signal with respect to the analyte concentration. Consequently, this approach fails to account for matrix effects and cannot be considered a valid method for their mitigation.

It can thus be concluded that no degree of mathematical, or rather, arithmetic, manipulation can substitute for the critical information that would otherwise be obtained by constructing a (potentially nonlinear) calibration curve using multiple standards.

The approach used in this paper to overcome the issues related to the matrix effect in the analysis of phosphorus in SSA relies on the use of an innovative non-linear multivariate approach, as described in the following section.

The use of advanced machine learning tools has become an essential part of the route of the LIBS technique towards its assessment as an established analytical technique [20]. The high complexity of LIBS spectra and the large amount of data generated in analytical applications call for advanced processing techniques capable of handling data often affected by matrix effects, spectral interferences, non-linearities, and random fluctuations. Neural networks, thanks to their robustness and ability to model non-linear relationships between input and output data, are ideal tools for accurately analyzing and classifying LIBS spectra.

Neural networks can significantly improve the precision and trueness of LIBS quantitative analysis by reducing the effects caused by variations in the sample matrix, plasma parameters (such as ablated mass, electron temperature, and number density), and environmental conditions. A well-trained ANN typically provides more robust calibrations than uni- or multivariate linear models, owing to its superior ability to manage the intrinsic complexity of the LIBS signal.

Compared to CF-LIBS, ANNs has the advantage of not requiring strict experimental conditions. For example, plasma LTE conditions are not necessary for quantitative analysis, which enables the use of compact time-integrated spectrometers—such as those employed in our case—that would not be suitable for a CF-LIBS approach.

The application of ANNs for the analysis of LIBS spectra was first proposed by Motto-Ros et al. [21] in 2008; more generally, among the many papers dealing with machine learning applications in LIBS, it's probably worth mentioning the proficiency contest organized by the French LIBS community [22] in 2018 and the two contests organized by the Brno LIBS group at the 10th Euro-Mediterranean Symposium on LIBS [23] and at the 12th LIBS international conference held in 2022 in Bari, Italy [24]. These proficiency contests have contributed to definitively assessing the importance of using machine learning tools for classification and quantification of complex samples by LIBS.

The recent introduction of deep learning algorithms in LIBS analysis, such as CNNs, has further expanded the analytical capabilities of the technique, enabling the automatic recognition of complex spectral patterns and thereby improving its classification and quantification performance in many applications [25–28].

2. Materials and methods

LIBS analysis was performed on SSA samples collected from two different waste-to-energy plants located in Northern Italy operating sewage sludge mono combustion; the phosphorus concentration in the samples was independently determined. Samples G1, G2, and G3 were analyzed by X-ray fluorescence (XRF) according to the UNI EN 15309 standard. Samples D1 and D2 were analyzed based on ICP-OES analysis after microwave digestion [29,30]. The nominal P concentrations are reported in Table 1.

Standards have been homogenized with a vortex mixer for 2–3 min, and then they were pressed into pellets (1 cm in diameter and a few millimeters thick) using a hydraulic press at 300 bar for approximately 5 min. The samples were analyzed using a SciAps Z-903 handheld LIBS instrument. This device is equipped with a diode-pumped Nd:YAG laser, delivering 6 mJ at 1064 nm with a pulse duration of 1 ns (Full Width at Half Maximum). The laser beam is focused onto the sample with a spot size of 100 μm. The LIBS signal is collected over a spectral range from 150 nm to 950 nm using three spectrometers, each coupled to a time-integrated CCD with a gate time of 3 ms. The spectral resolution is 0.18 nm from 150 to 365 nm, 0.24 nm from 365 to 620 nm, and 0.35 nm from 620 to 950 nm. The acquisition of the CCD signal can be appropriately delayed for reducing the continuum emission that dominates the early stages of plasma formation. All samples were measured in triplicate, with each region of analysis averaging 12 spectra. We assessed the sustainability of the handheld LIBS workflow using the AGREE metric (default equal weighting across the 12 Green Analytical Chemistry principles) [5]. Operationalization followed our experimental setup (at-line measurement; ~1 g bulk handled; ≤3 low-intensity prep steps with pressing; manual execution; no derivatization or reagents; waste limited to at most the bulk aliquot, which can alternatively be returned; ≥10 analytes possible; ~6 samples h^{-1} throughput; lower per-analysis energy demand than ICP-MS; no toxic solvents). The resulting overall AGREE score is 0.77, indicating a favorable greenness profile (see Fig. 1).

Quantitative analysis of the SSA samples was performed in MATLAB (R2025a) using a deep learning algorithm based on a Convolutional Neural Network (CNN). The potential advantages and drawbacks of using deep learning methods, such as CNNs, compared to conventional machine learning techniques based on 'shallow' Artificial Neural Networks (ANNs), have been discussed in detail in [31]. NNs offer a good balance between analytical performance and interpretability, as well as simplicity and computational efficiency—important factors considering the limited processing capabilities of handheld LIBS devices. Machine learning approaches using ANNs in combination with handheld instrumentation have previously been applied to the analysis of steel [32], and more recently, to the determination of lithium concentration in black

Table 1
Phosphorus weight percentage in the calibration samples and associated uncertainties, calculated from the weighed mass.

Calibration Sample #	Nominal mixing proportion (w%-w%) Na2HPO4·2H2O - CaCO3	P concentration (w%)
S1	2–98	0.4 ± 0.2
S2	4–96	0.7 ± 0.2
S3	6–94	1.0 ± 0.2
S4	8–92	1.4 ± 0.2
S5	10–90	1.8 ± 0.2
S6	12–88	2.1 ± 0.2
S7	15–85	2.6 ± 0.2
S8	20–80	3.5 ± 0.2
S9	25–75	4.3 ± 0.2
S10	30–70	5.2 ± 0.2
S11	35–65	6.1 ± 0.2
S12	40–60	6.96 ± 0.2
S13	45–55	7.8 ± 0.2
S14	50–50	8.7 ± 0.25
S15	55–45	9.6 ± 0.3
S16	60–40	10.4 ± 0.3
S17	65–35	11.3 ± 0.4
S18	70–30	12.2 ± 0.2

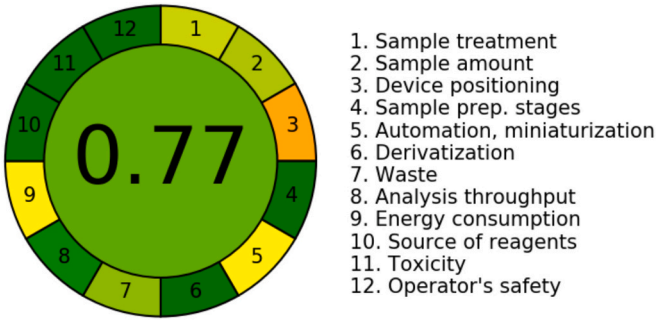

Fig. 1. The parameters used for calculating the AGREE score for the proposed methodology.

mass [33]. However, deep learning algorithms, particularly CNNs, offer a greater capacity for generalization when the training samples differ significantly in matrix composition from the samples being analyzed—precisely the challenge addressed in this study [34]. For this reason, we selected a deep learning approach and implemented a CNN with the same architecture as those successfully employed by Li et al. [35] for the quantitative analysis of minerals relevant to Martian geochemical exploration, and by Poggialini et al. [31] for the elemental analysis of bronze samples. The input to the CNN consisted of spectral data from the region below 220 nm, where the emission lines of iron are less dominant compared to longer wavelengths. This spectral region was chosen to minimize interference and improve the reliability of phosphorus quantification.

A key requirement for the effective application of CNNs is the availability of many training samples, each with multiple spectra. The eighteen standard samples used in this study, each analyzed at three different points, did not provide enough spectra for robust CNN training. To address this limitation and reduce the risk of overfitting, we applied data augmentation techniques as described in [31,36]. In particular, we used the 'bootstrap' method, which consists of randomly averaging the LIBS spectra obtained on a sample in groups of two or three. To obtain new spectra from the many possible independent combinations of the original spectra. This averaging procedure has the positive side effect of reducing the effects of outliers and improving the signal-to-noise ratio of the LIBS spectra. Moreover, we also digitally increased the number of training and test samples by averaging the LIBS spectra of different physical samples to simulate a new sample with a composition corresponding to the average composition of the two [31]. The latter procedure is not completely rigorous, because of the non-linear dependence of the LIBS signal on the sample composition. However, by averaging the spectra of samples with similar matrix, the errors due to this non-linearity remain at acceptable levels, as demonstrated by the good performances of the CNN approach for the determination of phosphorous concentration in the SSA samples.

This process resulted in the generation of over 25,000 spectra for both the reference and SSA samples—an amount sufficient to ensure the statistical reliability of the results. The block scheme of the CNN used is shown in Fig. 2.

For the training of the CNN we used the SDGM (Stochastic Gradient Descent with Momentum) solver. Over 20,000 spectra from the synthetic samples augmented dataset for training and about 3500 spectra from the SSA augmented dataset for validation were used, with a validation frequency set to 50. The maximum number of epochs was set to 4, with 370 iteration per epoch and a mini-batch of 64 observations at each iteration. The initial learning rate was set to 10^{-3} and the learning rate drop factor to 0.1, with a learning rate drop period of 20. L2 regularization was employed, with a factor of 10^{-4}. An early stop condition of RMSE <0.001 was applied.

The input layer takes the spectral data in the region below 220 nm (about 500 'pixels', i.e. spectral points) in the form of 1-D array. The first convolution step applies to 8 filters, 10 pixels wide, with a step (stride) of 2. The resulting 2D array is normalized before applying a ReLU (rectified linear activation function). A pooling layer operates a reduction of the number of points picking the maximum of the array in a region of four points, with a step of two points. A second step of convolution, normalization, ReLU and pooling further reduced the size of the matrix. Finally, a sequence of three convolutions, normalization and ReLU layers selects the input points, which are fed to a fully connected layer with an output size of 1024, which become the inputs of the final fully connected layer, providing the calculated P mass concentration.

The main issue with this approach is the generalization capability of the model, built using reference samples, to the more complex matrix of real SSA samples.

In training an ANN or CNN, it is customary to divide the data acquired from calibration samples into three groups: training, validation, and test sets. After building the model, it must be further validated using data that were not included in the previous steps (external validation).

Our strategy involved training the CNN on the (augmented) reference samples and validating it using the (augmented) SSA samples. This approach satisfies the essential requirement of external validation with samples not included in the training phase [31], while also allowing the selection of spectral features less affected by matrix differences between the reference and real SSA samples. In this way, we obtained a model that is general enough to accurately represent both the calibration and real samples, while also achieving external validation, since only the calibration samples were used for model construction and the SSC samples were exclusively used for testing.

From an operational perspective, many models were tested. The criterion for selecting the final CNN structure was the minimization of the Root Mean Square Error (RMSE) between the CNN predictions and the nominal phosphorus concentrations in the SSA validation samples.

The training and optimization of CNN is a relatively time-consuming and computationally intensive process. On the medium-performance laptop with a GPU used for this work, the optimization process took approximately one hour. However, since the training can be performed offline, the final model can be easily transferred to the LIBS instrument's internal computer, enabling real-time determination of phosphorus content in SSA.

3. Results

LIBS spectra obtained using the hand-held instrument on the SSA samples are extremely rich in emission lines, as shown in Fig. 3.

The portion of the spectrum above 220 nm is heavily dominated by Fe I and Fe II emission lines, along with several intense lines of Ca I and Ca II, including the prominent resonance lines at 393.4 nm and 396.8 nm. This region also includes the sodium doublet at 589.0 nm and 589.6 nm, as well as emission lines from lithium, magnesium, titanium, potassium, silicon, and many other elements. Due to the high degree of spectral crowding and interference, this region is not suitable for phosphorus quantification.

In contrast, the spectral region below 220 nm exhibits low interference from iron or other elements, making it suitable for the phosphorus analysis. In this region, several phosphorus emission lines are clearly observable, with the most intense lines appearing at 203.3 nm, 213.5 nm, 213.6 nm, 214.9 nm, and 215.4 nm. Additionally, the carbon line at 192.9 nm is present. Emission lines from neutral iron and magnesium and neutral and ionized silicon detectable in this region do not interfere with phosphorus (Fig. 4), allowing for reliable signal analysis of phosphorus lines.

The comparison of the SSA spectra with those obtained from the calibration samples evidence that the SSA samples have a high complex composition with respect to the laboratory-built reference samples, which only show carbon, phosphorous, sodium and (at longer wavelengths) calcium lines. The challenge in this case is to use the reference

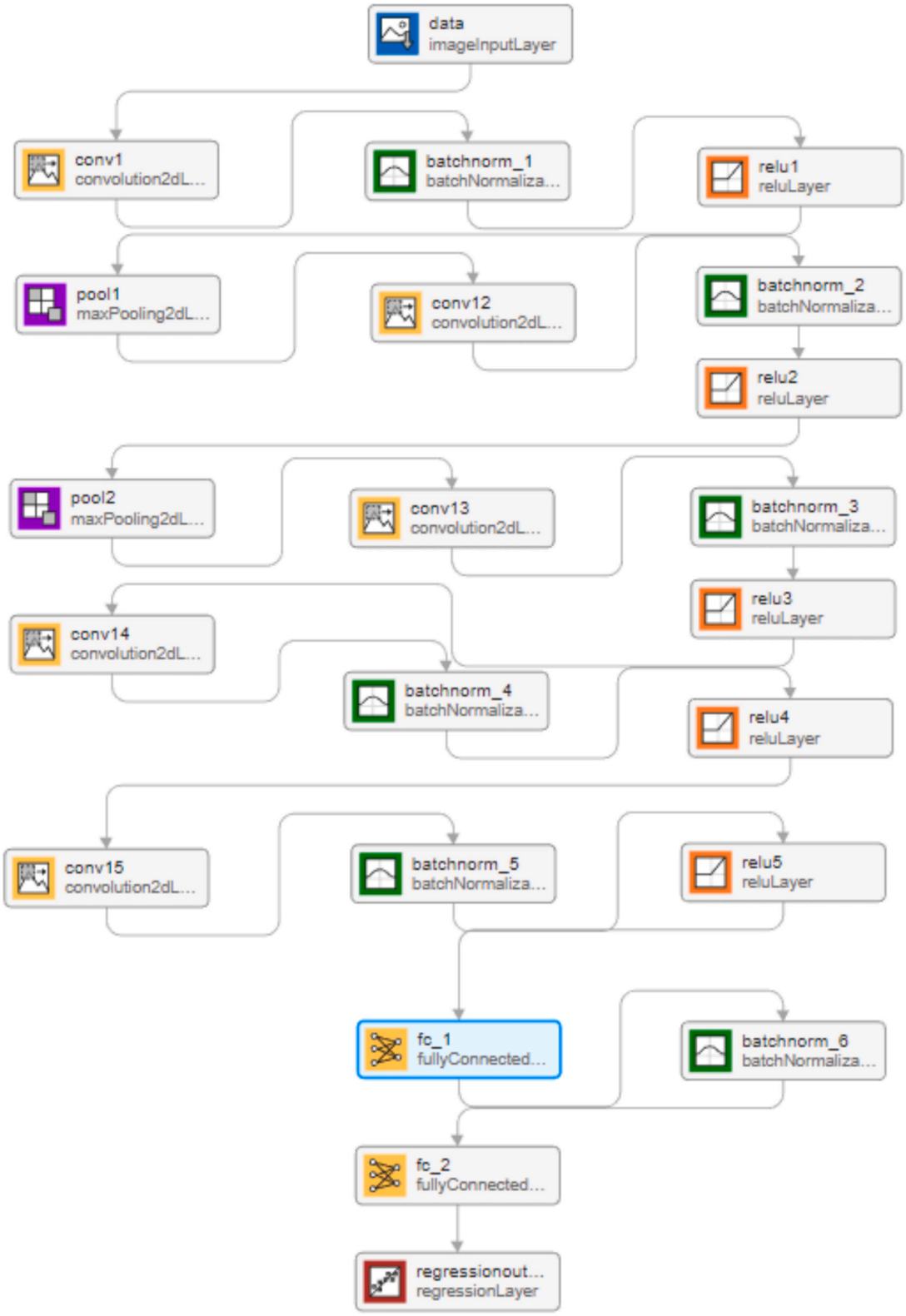

Fig. 2. Block scheme of the Convolutional Neural Network used in this paper.

samples to obtain a calibration procedure that would work well with them but would also be generalizable to the real-world samples.

To understand the challenge of this task, as a preliminary test, we built a conventional univariate calibration curve using reference samples. We used the integrated intensity of the most intense P I emission line at 203.3 nm, normalized to the integrated intensity of the entire spectrum. The predicted phosphorus concentration is plotted in Fig. 5 as a function of the phosphorus weight concentration in the samples.

In Figs. 5 to 7, the results obtained from three different points on the same calibration samples are treated as independent measurements. In this way, the spread among the points corresponding to the same sample (and therefore to the same phosphorus concentration) visually

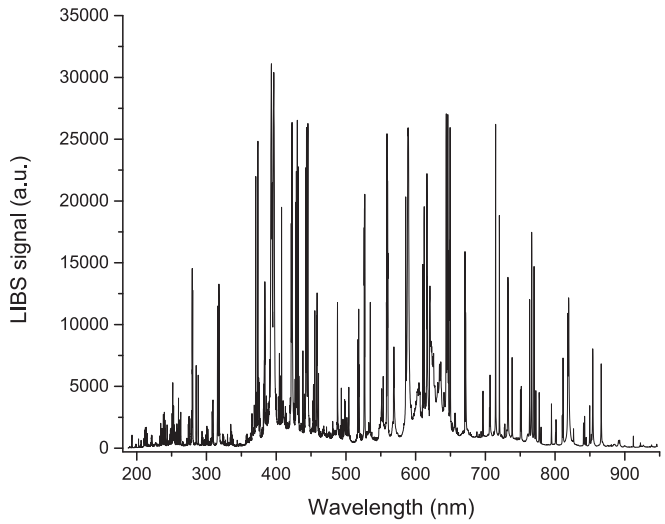

Fig. 3. LIBS spectrum taken on sample G1.

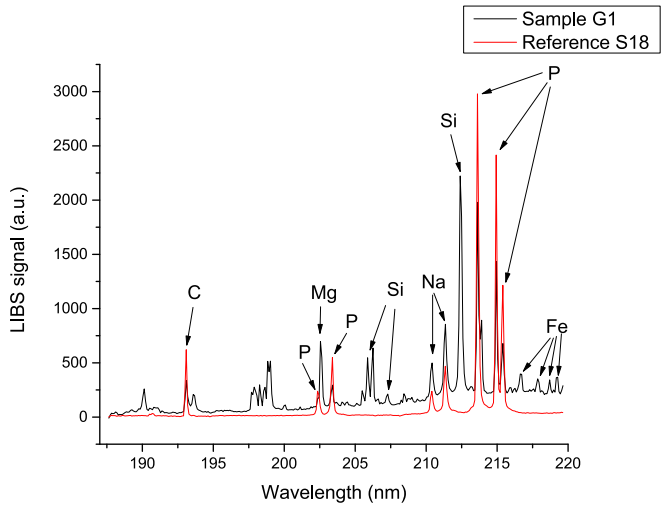

Fig. 4. Short wavelength portion of the LIBS spectrum of sample G1 (black) and reference sample S18 (red). (For interpretation of the references to colour in this figure legend, the reader is referred to the web version of this article.)

represents the uncertainty in the estimation of phosphorous concentration. For the SSC samples, we reported in the plot the average of the estimated values with y-error bars calculated as the standard deviation of the three independent measurements, while the uncertainty about their concentration was represented as x-error bar.

Although the calibration curve in Fig. 5 appears scattered, it shows a reasonably linear trend and adequately reflects the relationship between line intensity and phosphorous concentration in the reference samples. Normalizing the line intensity by the total spectrum intensity (roughly proportional to the ablated mass) helps compensate for the physical matrix effect associated with variations in ablated mass.

However, applying the above calibration curve to estimate phosphorus concentration in the SSA samples (Fig. 5 and Table 2) yields unreliable results.

This clearly indicates that a simple univariate model is insufficient to develop a generalized approach applicable to SSA samples. Similarly, a conventional machine learning approach would produce a calibration model largely unaffected by matrix differences among the reference samples. However, its performance would be limited when applied to the SSA samples due to the presence of numerous elements in the real samples that are absent from the standards. To highlight these

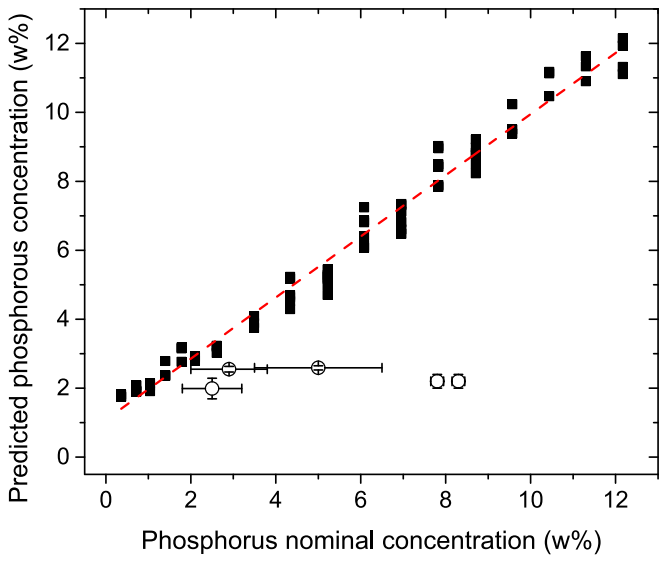

Fig. 5. Univariate calibration curve for phosphorus (black squares) and estimated concentrations of the SSA samples (white circles). Horizontal error bars represent the estimated uncertainties in the phosphorus weight concentration of the SSA samples.

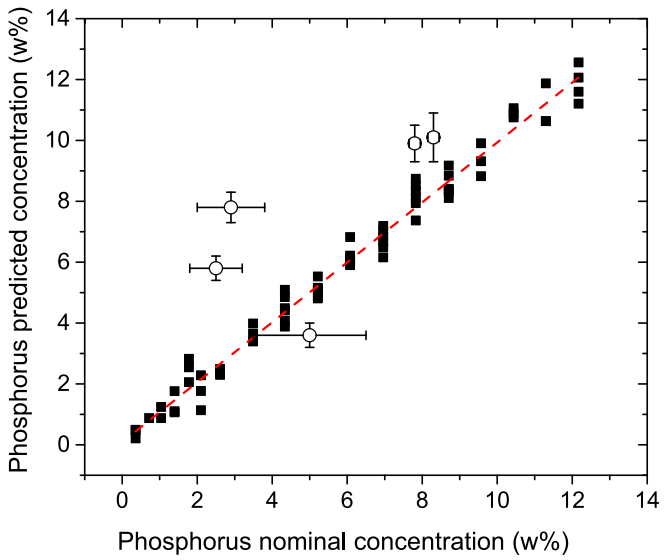

Fig. 6. ANN predicted vs. nominal phosphorus concentration for the reference samples (black squares) and the SSA samples (white circles). Horizontal error bars represent the estimated uncertainties in the phosphorus weight concentration of the SSA samples.

challenges, an artificial neural network (ANN) with the same architecture recently employed for the accurate determination of lithium in black mass using the same handheld instrument, comprising a single hidden layer with three neurons and an exponential activation function, was applied to the phosphorus samples [33]. The choice of the activation function and of the number of neurons in the hidden layer was performed using the ANN optimization tool of the software *Statistica* (ver. 8.0). After testing several models, with the number of neurons varying from 2 to 6, we decided to fix the number of neurons in the hidden layer to 3 to keep the number of neurons in the hidden layer as low as possible and, consequently, minimize the risk of overfitting. The optimized ANN achieves an acceptable fit for the reference samples (Fig. 6); however, its analytical performance on the actual SSA samples is clearly inadequate (Fig. 6 and Table 2).

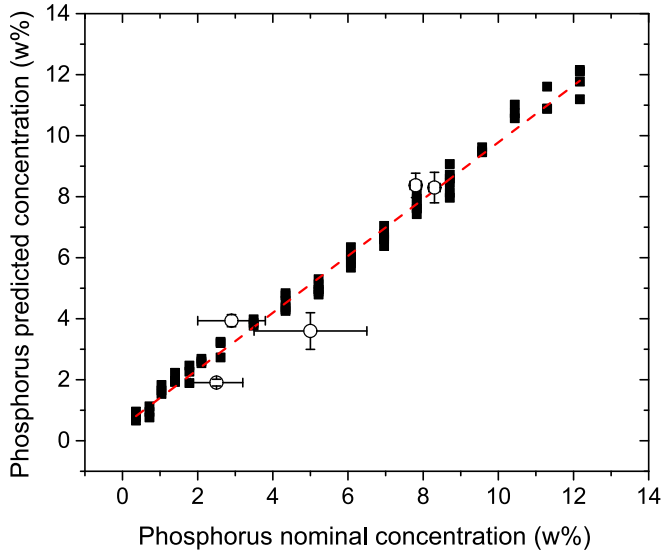

Fig. 7. CNN-predicted vs. nominal phosphorus concentrations for the reference samples (black squares) and SSA samples (white circles). Horizontal error bars represent the estimated uncertainties in the phosphorus weight concentration of the SSA samples.

Table 2
Nominal and predicted P concentration in SSA as calculated using univariate calibration, ANN, and CNN.

SSA Sample	Nominal P concentration (w%)	Univariate calibration (w%)	ANN (w %)	CNN (w %)
G1	2.9 ± 0.9	2.55 ± 0.04	7.8 ± 0.5	3.9 ± 0.2
G2	5 ± 1.5	2.59 ± 0.03	3.6 ± 0.4	3.6 ± 0.6
G3	2.5 ± 0.7	1.99 ± 0.2	5.8 ± 0.4	1.9 ± 0.1
D1	7.8 ± 0.15	2.2 ± 0.1	9.9 ± 0.6	8.4 ± 0.4
D2	8.3 ± 0.15	2.2 ± 0.1	10.1 ± 0.8	8.3 ± 0.5

On the other hand, the deep learning approach based on the CNN described above not only accurately predicts the phosphorus concentration in the reference samples (Fig. 7) but also demonstrates strong performance in predicting phosphorus levels in the SSA samples (Fig. 7 and Table 2), despite the latter having a complex matrix that differs significantly from that of the reference samples.

The analytical factors of merit of the of CNN vs. univariate calibration and classical ANN approach are reported in Table 3. The CNN approach is clearly superior to the latter, in terms of coefficient of determination (R^2), slope and intercept (bias) of the predicted vs. nominal concentration curve, as well as Root Mean Square Error of Prediction (RMSEP), defined as:

$$RMSEP = \sqrt{\frac{\sum (C_{LIBS} - C_{conv})^2}{N}} \quad (2)$$

where C_{LIBS} is the phosphorous concentration of the SSA samples determined by LIBS, C_{conv} is the phosphorous concentration determined by more conventional methods (XRF for samples G1, G2, and G3 or ICP-MS for samples D1 and D2) and N is the number of samples.

4. Conclusions

In this study, we presented a deep learning methodology for the in situ, rapid, and accurate determination of phosphorus content in SSA using a handheld LIBS instrument. The proposed method stands out for requiring minimal sample preparation and demonstrating a strong robustness to the severe matrix effects that typically hinder the accuracy of conventional LIBS analysis when applied to complex materials such as SSA.

Table 3
Analytical factors of merit of the three approaches tested in this paper.

	Slope	Bias (w%)	R^2	RMSEP (w%)
Univariate calibration	−0.01	2.4	0.02	3.9
ANN	0.49	4.2	0.16	3.0
CNN	1.11	−0.6	0.96	0.9

The core of the methodology is based on a Convolutional Neural Network (CNN), trained on LIBS spectra acquired from synthetic reference samples with well-defined phosphorus concentrations. To enhance the model's generalization capability, the training data were augmented to increase spectral variability. Validation was performed using spectra from a small set of independently characterized SSA samples, which present a considerably more complex and variable matrix than the reference standards, thus providing a rigorous test of the model's practical applicability.

The structure of the CNN was optimized by minimizing the root mean square error between predicted and actual phosphorus concentrations in the validation SSA samples. This strategy ensured that the model not only provided a good fit to reference data but also delivered accurate predictions under real-world conditions. Remarkably, the final model exhibited strong predictive performance on both the reference and SSA samples, suggesting that it effectively captured spectral features that are resilient to variations in matrix composition.

The training and optimization of the CNN, though computationally intensive, was completed in approximately one hour using a mid-range laptop equipped with a graphic processing unit. Since this process can be carried out offline, the finalized model can be easily transferred to the onboard computer of the LIBS instrument, enabling real-time, in-field analysis of phosphorus content in SSA without requiring complex preprocessing or laboratory infrastructure.

Finally, from a sustainability point of view, the AGREE assessment reflects the greenness of the proposed analytical method based on handheld LIBS.

CRediT authorship contribution statement

Mattia Massa: Investigation, Data curation. **Elisa Galli:** Investigation, Data curation. **Alessandra Zanoletti:** Supervision. **Annalisa Zacco:** Supervision. **Silvana De Iuliis:** Visualization. **Laura Eleonora Depero:** Writing – review & editing, Methodology, Conceptualization. **Vincenzo Palleschi:** Writing – review & editing, Writing – original draft, Software, Methodology, Formal analysis, Data curation. **Laura Borgese:** Writing – review & editing, Supervision, Methodology, Conceptualization. **Elza Bontempi:** Writing – review & editing, Resources, Methodology, Funding acquisition, Conceptualization.

Declaration of competing interest

The authors have no conflict of interest to declare.

Acknowledgements

This work was supported by F.O.S.F.O.R.O (Fanghi Organici Sostenibili per il Futuro: Ottimizzazione del Recupero di Ortofosfati e altri nutrienti, CUP: E89I25001040007), co-financed by Regione Lombardia, *European Union and ERDF.*

Alessandra Zanoletti acknowledges financial support from the Next-GenerationEU (Italian PNRR – M4 C2, Invest 1.3 – D.D. 1551.11-10-

2022, PE00000004 CUP D73C22001250001) within the MICS (Made in Italy Circular and Sustainable) Extended Partnership for her research fellowship.

The authors thank SciAps for providing the hand-held LIBS instrument used in this work.

Data availability

Data will be made available on request.

References

[1] H. Liu, G. Hu, I.A. Basar, J. Li, N. Lyczko, A. Nzihou, C. Eskicioglu, Phosphorus recovery from municipal sludge-derived ash and hydrochar through wet-chemical technology: a review towards sustainable waste management, Chem. Eng. J. 417 (2021) 129300, https://doi.org/10.1016/j.cej.2021.129300.

[2] S. Ducoli, A. Zacco, E. Bontempi, Incineration of sewage sludge and recovery of residue ash as building material: a valuable option as a consequence of the COVID-19 pandemic, J. Environ. Manag. 282 (2021) 111966, https://doi.org/10.1016/j.jenvman.2021.111966.

[3] L. Reijnders, Phosphorus resources, their depletion and conservation, a review, Resour. Conserv. Recycl. 93 (2014) 32–49, https://doi.org/10.1016/j.resconrec.2014.09.006.

[4] S. Papuga, M. Kotur, Resources efficient and cleaner production in the bentonite industry, Environ. Prog. Sustain. Energy 42 (2023), https://doi.org/10.1002/ep.14138.

[5] F. Pena-Pereira, W. Wojnowski, M. Tobiszewski, AGREE—analytical GREEnness metric approach and software, Anal. Chem. 92 (2020) 10076–10082, https://doi.org/10.1021/ACS.ANALCHEM.0C01887.

[6] E. Marguí, I. Queralt, E. de Almeida, X-ray fluorescence spectrometry for environmental analysis: basic principles, instrumentation, applications and recent trends, Chemosphere 303 (2022) 135006, https://doi.org/10.1016/J.CHEMOSPHERE.2022.135006.

[7] D.A. Cremers, L.J. Radziemski, Handbook of Laser-Induced Breakdown Spectroscopy, John Wiley & Sons, Ltd, Chichester, UK, 2006, https://doi.org/10.1002/0470093013.

[8] G.S. Senesi, R.S. Harmon, R.R. Hark, Field-portable and handheld laser-induced breakdown spectroscopy: historical review, current status and future prospects, Spectrochim. Acta Part B At. Spectrosc. 175 (2021), https://doi.org/10.1016/J.SAB.2020.106013.

[9] Laser-induced breakdown spectroscopy, Nat. Rev. Methods Primers 5 (2025) 18, https://doi.org/10.1038/s43586-025-00398-8.

[10] E. Tognoni, V. Palleschi, M. Corsi, G. Cristoforetti, Quantitative micro-analysis by laser-induced breakdown spectroscopy: a review of the experimental approaches, Spectrochim. Acta Part B At. Spectrosc. 57 (2002) 1115–1130, https://doi.org/10.1016/S0584-8547(02)00053-8.

[11] K. Elsayed, W. Tawfik, A.E.M. Khater, T.S. Kayed, M. Fikry, Fast determination of phosphorus concentration in phosphogypsum waste using calibration-free LIBS in air and helium, Opt. Quant. Electron. 54 (2022) 96, https://doi.org/10.1007/s11082-021-03474-x.

[12] A. Ciucci, M. Corsi, V. Palleschi, S. Rastelli, A. Salvetti, E. Tognoni, New procedure for quantitative elemental analysis by laser-induced plasma spectroscopy, Appl. Spectrosc. 53 (1999) 960–964, https://doi.org/10.1366/0003702991947612.

[13] G. Cristoforetti, A. De Giacomo, M. Dell'Aglio, S. Legnaioli, E. Tognoni, V. Palleschi, N. Omenetto, Local thermodynamic equilibrium in laser-induced breakdown spectroscopy: beyond the McWhirter criterion, Spectrochim. Acta Part B At. Spectrosc. 65 (2010) 86–95, https://doi.org/10.1016/j.sab.2009.11.005.

[14] F. Poggialini, B. Campanella, B. Cocciaro, G. Lorenzetti, V. Palleschi, S. Legnaioli, Catching up on calibration-free LIBS, J. Anal. At. Spectrom. 38 (2023) 1751–1771, https://doi.org/10.1039/D3JA00130J.

[15] E. Grifoni, S. Legnaioli, M. Lezzerini, G. Lorenzetti, S. Pagnotta, V. Palleschi, Extracting time-resolved information from time-integrated laser-induced breakdown spectra, J. Spectrosc. 2014 (2014), https://doi.org/10.1155/2014/849310.

[16] N. Lellouche, B. Cocciaro, S. Legnaioli, G. Lorenzetti, V. Palleschi, F. Poggialini, S. Raneri, S.M. Aberkane, A new method for calibration-free analysis by laser-induced breakdown spectroscopy using a time-integrated spectrometer, Spectrochim. Acta Part B At. Spectrosc. 215 (2024) 106903, https://doi.org/10.1016/j.sab.2024.106903.

[17] D.V. Babos, A.I. Barros, J.A. Nóbrega, E.R. Pereira-Filho, Calibration strategies to overcome matrix effects in laser-induced breakdown spectroscopy: direct calcium and phosphorus determination in solid mineral supplements, Spectrochim. Acta Part B At. Spectrosc. 155 (2019) 90–98, https://doi.org/10.1016/j.sab.2019.03.010.

[18] D.V. Babos, A. Virgilio, V.C. Costa, G.L. Donati, E.R. Pereira-Filho, Multi-energy calibration (MEC) applied to laser-induced breakdown spectroscopy (LIBS), J. Anal. At. Spectrom. 33 (2018) 1753–1762, https://doi.org/10.1039/C8JA00109J.

[19] V. Costa, D. Babos, J. Castro, D. Andrade, R. Gamela, R. Machado, M. Sperança, A. Araújo, J. Garcia, E. Pereira-Filho, Calibration strategies applied to laser-induced breakdown spectroscopy: a critical review of advances and challenges, J. Braz. Chem. Soc. (2021), https://doi.org/10.21577/0103-5053.20200175.

[20] V. Palleschi, Chemometrics and Numerical Methods in LIBS, John Wiley, 2022.

[21] V. Motto-Ros, A.S. Koujelev, G.R. Osinski, A.E. Dudelzak, Quantitative multi-elemental laser-induced breakdown spectroscopy using artificial neural networks, J. Eur. Opt. Soc. 3 (2008) 1–5.

[22] V. Motto-Ros, D. Syvilay, L. Bassel, E. Negre, F. Trichard, F. Pelascini, J. El Haddad, A. Harhira, S. Moncayo, J. Picard, D. Devismes, B. Bousquet, Critical aspects of data analysis for quantification in laser-induced breakdown spectroscopy, Spectrochim. Acta Part B At. Spectrosc. 140 (2018) 54–64, https://doi.org/10.1016/J.SAB.2017.12.004.

[23] J. Vrábel, E. Képeš, L. Duponchel, V. Motto-Ros, C. Fabre, S. Connemann, F. Schreckenberg, P. Prasse, D. Riebe, R. Junjuri, M.K. Gundawar, X. Tan, P. Pořízka, J. Kaiser, Classification of challenging laser-induced breakdown spectroscopy soil sample data - EMSLIBS contest, Spectrochim. Acta Part B At. Spectrosc. 169 (2020) 105872, https://doi.org/10.1016/j.sab.2020.105872.

[24] E. Képeš, J. Vrábel, P. Siozos, V. Pinon, P. Pavlidis, D. Anglos, T. Chen, L. Sun, G. Lu, D.J. Díaz-Romero, S. Van den Eynde, I. Zaplana, J. Peeters, V. Kaňa, A. Záděra, V. Palleschi, A. De Giacomo, P. Pořízka, J. Kaiser, Quantification of alloying elements in steel targets: the LIBS 2022 regression contest, Spectrochim. Acta Part B At. Spectrosc. 206 (2023) 106710, https://doi.org/10.1016/J.SAB.2023.106710.

[25] W. Huang, L. Guo, W. Kou, D. Zhang, Z. Hu, F. Chen, Y. Chu, W. Cheng, Identification of adulterated milk powder based on convolutional neural network and laser-induced breakdown spectroscopy, Microchem. J. 176 (2022) 107190, https://doi.org/10.1016/j.microc.2022.107190.

[26] J. Chen, J. Pisonero, S. Chen, X. Wang, Q. Fan, Y. Duan, Convolutional neural network as a novel classification approach for laser induced breakdown spectroscopy applications in lithological recognition, Spectrochim. Acta Part B At. Spectrosc. 166 (2020) 105801.

[27] P. Xing, J. Dong, P. Yu, H. Zheng, X. Liu, S. Hu, Z. Zhu, Quantitative analysis of lithium in brine by laser-induced breakdown spectroscopy based on convolutional neural network, Anal. Chim. Acta 1178 (2021) 338799, https://doi.org/10.1016/j.aca.2021.338799.

[28] P. Khalilian, F. Rezaei, N. Darkhal, P. Karimi, A. Safi, V. Palleschi, N. Melikechi, S. H. Tavassoli, Jewelry rock discrimination as interpretable data using laser-induced breakdown spectroscopy and a convolutional LSTM deep learning algorithm, Sci. Rep. 14 (2024) 5169, https://doi.org/10.1038/s41598-024-55502-x.

[29] M. Massa, S. Calce, P. Pachaiappan, B. Valentim, C. Punta, A. D'Anna, M. Blazina, E. Bontempi, Exploring the potential of sewage sludge ash for CO2 sequestration and resource recovery, J Water Process Eng 71 (2025) 107153, https://doi.org/10.1016/j.jwpe.2025.107153.

[30] M. Massa, A. Zanoletti, L. Fiameni, B. Valentim, L.E. Depero, E. Bontempi, Improving phosphorus availability in sewage sludge ash through a novel microwave-based technology, Water Environ. J. 39 (2025) 35–46, https://doi.org/10.1111/wej.12956.

[31] F. Poggialini, B. Campanella, S. Legnaioli, S. Raneri, V. Palleschi, Comparison of convolutional and conventional artificial neural networks for laser-induced breakdown spectroscopy quantitative analysis, Appl. Spectrosc. 2022 (2022) 959–966, https://doi.org/10.1177/00037028221091300/ASSET/IMAGES/LARGE/10.1177_00037028221091300-FIG 1.JPEG.

[32] F. Poggialini, B. Campanella, S. Legnaioli, S. Pagnotta, S. Raneri, V. Palleschi, Improvement of the performances of a commercial hand-held laser-induced breakdown spectroscopy instrument for steel analysis using multiple artificial neural networks, Rev. Sci. Instrum. 91 (2020) 073111, https://doi.org/10.1063/5.0012669.

[33] E. Galli, M. Massa, A. Zanoletti, S. De Iuliis, E. Bontempi, L.E. Depero, V. Palleschi, L. Borgese, Determination of lithium concentration in black mass using laser-induced breakdown spectroscopy hand-held instrumentation, Sci. Rep. 15 (2025) 17483, https://doi.org/10.1038/s41598-025-90379-4.

[34] U. Michelucci, Fundamentals of convolutional neural networks, in: Advanced Applied Deep Learning, Apress, 2019, pp. 79–123, https://doi.org/10.1007/978-1-4842-4976-5_3.

[35] L.N. Li, X.F. Liu, W.M. Xu, J.Y. Wang, R. Shu, A laser-induced breakdown spectroscopy multi-component quantitative analytical method based on a deep convolutional neural network, Spectrochim. Acta Part B At. Spectrosc. 169 (2020), https://doi.org/10.1016/j.sab.2020.105850.

[36] E. Képeš, P. Pořízka, J. Kaiser, On the application of bootstrapping to laser-induced breakdown spectroscopy data, J. Anal. At. Spectrom. 34 (2019) 2411–2419, https://doi.org/10.1039/C9JA00304E.doi:10.1038/s41598-017-03426-0.